Available online at www.sciencedirect.com
ScienceDirect
Acta Materialia 57 (2009) 1938–1946
Acta MATERIALIA
www.elsevier.com/locate/actamat

A new organic/inorganic electroluminescent material with a silsesquioxane core

Chih-Chia Cheng [a], Chen-Han Chien [a], Ying-Chieh Yen [a], Yun-Sheng Ye [a], Fu-Hsiang Ko [b], Chun-Hung Lin [c], Feng-Chih Chang [a,*]

[a] *Institute of Applied Chemistry, National Chiao-Tung University, 30050 Hsinchu, Taiwan*
[b] *Institute of Nanotechnology, National Chiao-Tung University, 30050 Hsinchu, Taiwan*
[c] *Institute of Electro-Optical and Science and Engineering, National Cheng Kung University, 70101 Tainan, Taiwan*

Received 24 September 2008; received in revised form 28 December 2008; accepted 30 December 2008
Available online 11 February 2009

Abstract

This paper describes a new polyhedral oligomeric silsesquioxane (POSS)-based blue-light electroluminescent nanoparticle, octakis[*N*-(9-ethyl-9*H*-carbazol-3-yl)undecanamide-11-dimethylsiloxy]silsesquioxane (POSS-C11-Cz), which contains eight carbazole chromophore arms, synthesized through the hydrosilation reaction of octakis(dimethylsiloxy)silsesquioxane with the terminal olefin Cz-C11ene. POSS-C11-Cz exhibits good thermal and electrochemical stabilities and good film-forming properties. The optical and photoluminescence spectra of POSS-C11-Cz in solution and in the solid state indicate a reduction in the degrees of aggregation and excimer formation because inter-chain interactions were prohibited by the bulky POSS core. Moreover, photoluminescence spectra of a POSS-C11-Cz (3 wt.%)/polyfluorene (97 wt.%) blend revealed that the color was stable after heating the sample at 200 °C for 5 h; in contrast, the pure polyfluorene exhibited a significant green emission at 530 nm. A triple-layer device based on this blend exhibited higher maximum brightness and luminance efficiencies relative to those of the pure polyfluorene. Thus, the organic/inorganic POSS-C11-Cz/polyfluorene blend has potential for use in polymeric light-emitting diodes because of its improved thermal and optoelectronic characteristics.
Published by Elsevier Ltd on behalf of Acta Materialia Inc.

Keywords: Polymer matrix composites; Nanocomposite; Optical materials; Blending

1. Introduction

Polyhedral oligomeric silsesquioxanes (POSSs), $(RSiO_{1.5})_n$, are intermediates between silica (SiO_2) and silicone (R_2SiO); they comprise a hydrophobic inorganic core covered externally by organic substituents [1–6]. Recently, organic/inorganic hybrid nanocomposites based on POSS derivatives have attracted considerable interest [7–10] because they exhibit several advantageous properties resulting from the unique physical properties of POSS nanoparticles (NPs) [1,2,11–13]. Through appropriate design of their architectures, POSS derivatives can be tailored for specific applications [14–16]. The presence of POSS derivatives can improve quantum efficiencies, improve the thermal stability of conjugated polymers, suppress the aggregation of conjugated groups, and enhance photoluminescence (PL) and electroluminescence (EL) performance [17–22].

Sellinger et al. [21,23] used Heck coupling to synthesize a POSS derivative containing eight octavinyl groups and explored its application in electroluminescent devices. Jabbour et al. [24] and Shim et al. [22] synthesized POSS derivatives containing eight chromophore groups and reported that they enhanced the EL emissive properties and quantum efficiencies of the host through energy transfer. Xiao et al. [25] used Grignard chemistry to synthesize an oligophenylene-functionalized POSS. Kawakami et al. [26] reported that a POSS derivative containing eight carbazole

* Corresponding author. Tel./fax: +886 3 5131512.
E-mail address: changfc@mail.nctu.edu.tw (F.-C. Chang).

1359-6454/$36.00 Published by Elsevier Ltd on behalf of Acta Materialia Inc.
doi:10.1016/j.actamat.2008.12.031

groups enhanced the PL properties of poly(9-vinylcarbazole) (PVK), but they did not develop it into an electroluminescent device.

In previous studies, we found that the incorporation of POSS derivatives improves the properties of several polymeric matrixes [27–32]. In this study, we prepared a new POSS derivative, POSS-C11-Cz, that contains eight 3,9-ethylcarbazole groups and exhibits good optical and electroluminescence properties and high electrochemical stability. The linkage of the carbazole units via alkyl chain spacers to the POSS cage suppresses their aggregation. POSS-C11-Cz is a blue light-emitting NP possessing a suitable glass transition temperature for fabrication into solid state devices; it enhances the color stability of blue light-emitting polyfluorenes through energy transfer [33–39].

2. Experimental

2.1. Materials

3-Amino-9-ethylcarbazole (AECz) was purchased from Acros Organics (USA) and recrystallized from cyclohexane. 10-Undecenoyl chloride and platinum-divinyltetramethyldisiloxane complex (Pt-dvs, the hydrosilylation catalyst) were obtained from Aldrich (USA). Octakis(dimethylsilyloxy)-POSS (Ot-POSS) was purchased from Hybrid Plastics (USA). Acryloyl chloride was purchased from Alfa Aesar (USA) and used as received. Poly(9,9′-dioctylfluorene) (POF) was synthesized through Suzuki coupling according to a procedure described previously [70,71]. Gel permeation chromatography (GPC) analysis indicated that the molecular weight of POF was ca. 20,000 g mol^{-1}, with a polydispersity index (PDI, M_w/M_n) of 1.2. All solvents were purchased from TEDIA (USA) and distilled over CaH_2 prior to use. All other chemicals were used as received without purification.

2.1.1. N-(9-Ethyl-carbazol-3-yl)undec-10-enamide (Cz-C11ene)

AECz (2 g, 9.5 mmol, 100 mol.%) and triethylamine (0.96 g, 9.5 mmol, 100 mol.%) were dissolved in dry tetrahydrofuran (THF, 60 ml) and then the mixture was cooled to 0 °C in an ice bath. A solution of 10-undecenoyl chloride (2.7 g, 14.3 mmol, 150 mol.%) in dry THF (20 ml) was added dropwise to this mixture over a period of 1 h; the reaction was left to proceed at 0 °C for 3 h and then at room temperature for an additional 8 h. Finally, the reaction mixture was filtered, the solvent evaporated and the residue purified through chromatography (SiO_2; 20% hexane/ethyl acetate) to give Cz-C11ene (3.18 g, 89%) as a gray powder. M.p.: 115 °C; ^{1}H nuclear magnetic resonance (NMR) (300 MHz, $CDCl_3$, 25 °C): $\delta = 8.30$ (s, 1H; NH), 8.06 (d, $J = 7.70$ Hz, 1H; Ar-CH), 7.51–7.10 (m, 7H; Ar-CH), 5.91–5.70 (m, 1H; CH), 4.97 (dd, $J_1 = 28.20$ Hz, $J_2 = 14.52$ Hz, 2H; CH_2), 4.31 (dd, $J = 7.17$, 14.34 Hz, 2H; CH_2), 2.40 (t, $J = 7.53$ Hz, 2H; CH_2), 2.05–1.98 (m, 2H; CH_2), 1.77-1.71 (m, 2H; CH_2), 1.49–1.20 (m, 13H; CH_2, CH_3) ppm; ^{13}C NMR (75 MHz, $CDCl_3$, 25 °C): $\delta = 171.5$, 160.6, 139.6, 137.28, 129.8, 125.9, 123.3, 120.8, 120.1, 118.8, 114.3, 113.0, 108.7, 108.4, 37.9, 37.7, 34.0, 29.5, 29.3, 29.1, 26.0, 14.0 ppm; LRMS (EI): m/z 376 $[M]^+$; elemental analysis: calcd (%) for $C_{25}H_{32}N_2O$: C, 79.75; H, 8.57; N, 7.44. Found: C, 79.07; H, 8.50; N, 7.61.

2.1.2. POSS-C11-Cz

A solution of Pt-dvs (0.1 ml, 200 ppm) was injected via syringe into a solution of Ot-POSS (0.51 g, 0.5 mmol, 100 mol.%) and Cz-C11ene (1.89 g, 5 mmol, 100 mol.%) in dry toluene (15 ml). The mixture was stirred at 80 °C under an argon atmosphere until the Si–H peak (2140 cm^{-1}) disappeared completely (2 h). After cooling to room temperature, the mixture was filtered and the solid washed several times with toluene and then dried under vacuum to yield POSS-C11-Cz (1.90 g, 95%); ^{1}H NMR (300 MHz, $CDCl_3$, 25 °C): $\delta = 8.23$ (br, 8H; NH), 8.06–7.90 (m, 8H; Ar-CH), 7.51–7.10 (m, 48H; Ar-CH), 4.13 (m,16H; CH_2), 2.40 (m,16H; CH_2), 1.73 (m,16H; CH_2), 1.28 (m, 136H; CH_2, CH_3), 0.60–0.42 (m, 16H; CH_2), 0.13 (m, 48H; CH_3) ppm; ^{13}C NMR (75 MHz, $CDCl_3$, 25 °C): $\delta = 171.5$, 160.6, 137.28, 129.8, 125.9, 123.3, 120.8, 120.1, 118.8, 113.0, 108.7, 108.4, 37.9, 37.7, 34.0, 29.5, 29.3, 29.1, 26.0, 23.3, 18.0, 14.0, 0.0 ppm; matrix-assisted laser desorption/ionization time-of-flight mass spectrometry (MALDI-TOF): m/z 4051.535 $[M + Na]^+$; elemental analysis: calcd (%) for $C_{216}H_{312}N_{16}O_{28}Si_{16}$: C, 64.37; H, 7.80; N, 5.56. Found: C, 64.08; H, 7.83; N, 5.29.

2.1.3. 3-Acrylamide-9-ethylcarbazole (AcrCz)

A solution of acryloyl chloride (1.3 g, 14.3 mmol, 150 mol.%) in dry THF (20 ml) was added dropwise over a period of 1 h to a solution of AECz (2 g, 9.5 mmol, 100 mol.%) and triethylamine (0.96 g, 9.5 mmol, 100 mol.%) in dry THF (60 ml) while cooling at 0 °C in an ice bath. The reaction mixture was stirred at 0 °C for 3 h and then at room temperature for an additional 8 h. After evaporating the solvent, the residue was partitioned between CH_2Cl_2 (100 ml) and 0.1 N sodium carbonate. The organic extract was dried ($MgSO_4$) and evaporated to dryness; the residue was purified through chromatography (SiO_2; 10% hexane/ethyl acetate) to give AcrCz (1.88 g, 75%) as a gray powder. M.p.: 179 °C; ^{1}H NMR (300 MHz, $CDCl_3$, 25 °C): $\delta = 8.38$ (s, 1H; NH), 8.04 (d, $J = 7.73$ Hz, 1H; Ar-CH), 7.78–7.15 (m, 6H; Ar-CH), 6.49 (d, $J = 7.73$ Hz, 1H; CH), 6.37–6.24 (dd, $J = 1.22$, 9.98 Hz, 1H; CH), 5.76 (d, $J = 7.73$ Hz, 1H, CH), 4.34 (dd, $J = 7.17$, 14.34 Hz, 2H; CH_2), 1.38 (m, 3H; CH_3) ppm; ^{13}C NMR (75 MHz, $CDCl_3$, 25 °C): $\delta = 163.8$, 150.6, 137.4, 131.6, 129.6, 127.4, 126.1, 123.2, 122.9, 120.9, 119.5, 119.0, 113.1, 108.7, 37.6, 14.0 ppm; LRMS (EI): m/z 264 $[M]^+$; elemental analysis: calcd (%) for $C_{17}H_{16}N_2O$: C, 77.25; H, 6.10; N, 10.60. Found: C, 76.60; H, 6.12; N, 10.27.

2.1.4. Poly(3-acrylamide-9-ethylcarbazole) (PACz)

A mixture of AcrCz (1 g, 3.8 mmol) and 2,2́-azobisisobutyronitrile (AIBN, initiator, 5 wt.%) was stirred at 140 °C in a mixture of dry *N*,*N*-dimethylformamide (DMF, 7 ml) and toluene (3 ml) under an argon atmosphere for 24 h. The product, PACz, was obtained as a slightly gray powder after precipitation into methanol. The molecular weight and the polydispersity index (PDI, weight-average molecular weight (M_w)/number-average molecular weight (M_n)) of the PACz polymer, obtained from GPC analysis, were ca. 20,000 g mol^{-1} and 2.04, respectively. Conversion: 96%; ^{1}H NMR (300 MHz, $CDCl_3$, 25 °C): $\delta = 8.38$ (br, NH), 8.04–6.19 (br, Ar-CH), 3.78 (br, CH_2), 2.07 (br, CH), 1.25 (br, CH_3), 0.89 (br, CH_2) ppm; elemental analysis: calcd (%) for C, 77.25; H, 6.10; N, 10.60. Found: C, 77.01; H, 6.24; N, 10.11.

2.2. Characterization

2.2.1. Nuclear magnetic resonance spectroscopy

^{1}H and ^{13}C NMR spectra were recorded at 300 and 75 MHz, respectively, using a Varian Inova 300 MHz spectrometer equipped with a 9.395-T Bruker magnet. The samples (ca. 5 mg for ^{1}H NMR; ca. 20 mg for ^{13}C NMR) were dissolved in deuterated solvent and analyzed at room temperature.

2.2.2. Gel permeation chromatography

The M_w, M_n and PDI (M_w/M_n) were measured using a Waters 410 GPC system equipped with a refractive index detector and three Ultrastyragel columns (100, 500, and 1000 Å) connected in series. DMF was the eluent; the flow rate was 0.6 ml min^{-1}. The system was calibrated using polystyrene standards.

2.2.3. Elemental analysis

The carbon, hydrogen and nitrogen atom contents of the samples were obtained using a CHN-O-Rapid elemental analyzer (Foss. Heraeus, Germany).

2.2.4. Gas chromatography/mass spectrometry

Gas chromatography/mass spectrometry spectra were acquired using a Micromass Trio 2000 mass spectrometer (Micromass, Beverly, MA).

2.2.5. Matrix-assisted laser desorption/ionization time-of-flight mass spectrometry

MALDI-TOF mass spectra were recorded using a Bruker AutoFlex spectrometer equipped with a 337 nm N_2 laser (over 20 Hz).

2.2.6. Thermogravimetric analysis

Thermogravimetric analysis (TGA) was performed using a TA Instruments TGA 2050 thermogravimetric analyzer operated at a heating rate of 20 °C min^{-1} from room temperature to 800 °C under a continuous flow of nitrogen.

2.2.7. Differential scanning calorimetry

Differential scanning calorimetry (DSC) was performed using a DuPont 910 DSC-9000 controller operated under an atmosphere of dry N_2. The samples were weighed (ca. 5–10 mg) and sealed in an aluminum pan, then heated from −100 to +200 °C at a scan rate of 20 °C min^{-1}. The glass transition temperature was taken as the midpoint of the heat capacity transition between the upper and lower points of the deviation from the extrapolated glass and liquid lines.

2.2.8. Wide-angle X-ray diffraction

Wide-angle X-ray diffraction (WAXD) spectra of powders were obtained using a Rigaku D/max-2500 X-ray diffractometer. The radiation source was Ni-filtered Cu K_α radiation at a wavelength of 0.154 nm. The voltage and current were set at 30 kV and 20 Ma, respectively. The sample was mounted on a circular sample holder; the data were collected using a proportional counter detector over the 2θ range from 2° to 50° at a rate of 5° min^{-1}. Bragg's law ($\lambda = 2d \sin\theta$) was used to compute the *d*-spacing corresponding to the complementary behavior.

2.2.9. Scanning electron microscopy

Scanning electron microscopy (SEM) images were obtained using a JEOL-7401F field emission SEM microscope operated at 15 kV. The sample for SEM investigation was prepared by placing a drop of the sample solution onto a wafer and then evaporating the solvent (THF).

2.2.10. Cyclic voltammetry

Cyclic voltammetry was performed using a BAS 100 B/W electrochemical analyzer operated at a scanning rate of 100 mV s^{-1} in dichloromethane. Each sample contained 0.1 M tetrabutylammonium hexafluorophosphate as a supporting electrolyte in a cell equipped with a platinum working electrode. The potential were measured against an Ag/Ag^+ (0.01 M $AgNO_3$) reference electrode. Ferrocene was the internal standard.

2.2.11. Ultraviolet–visible and photoluminescence spectra

Ultraviolet–visible (UV–vis) and PL spectra were measured using an HP 8453 diode-array spectrophotometer and a Hitachi F-4500 luminescence spectrometer, respectively.

2.2.12. Light-emitting devices

Devices were fabricated in the configuration ITO/poly(3,4-ethylene dioxythiophene) (PEDOT, 35 nm)/polymer (ca. 60 nm)/1,3,5-tris(*N*-phenylbenzimidazol-2-yl)benzene (TPBI, 30 nm)/LiF (150 nm)/Al (100 nm). The PEDOT layer was used as a hole injection layer to facilitate hole conduction, and also to smoothen the relatively rough ITO layer. The TPBI layer deposited through thermal evaporation was employed as an electron-transporting

and hole-blocking layer. The device was characterized following procedures described previously [36,72].

3. Results and discussion

3.1. Synthesis and characterization of POSS-C11-Cz

We synthesized the electroluminescent NP POSS-C11-Cz through the hydrosilation reaction (Scheme 1) between octakis(dimethylsiloxy)silsesquioxane (Ot-POSS) and an allyl-functionalized Cz-C11ene, which functioned as a hole transporting organic semiconducting segment [40]. POSS-C11-Cz was recovered in high yield (95%) after direct filtration of the cooled mixture; its molecular weight ($M_w = 4028$) was consistent with the structure of the molecule presented in the Experimental section and in the Supporting information. In addition, we also synthesized an acrylic polymer, poly(3-acrylamide-9-ethyl-carbazole) (PACz), presenting the carbazole chromophore on its side chains [41]. POSS-C11-Cz exhibits good solubility in common organic solvents, such as THF, methylene chloride, chloroform and chlorobenzene. The formation of a film of POSS-C11-Cz through solvent-casting onto an indium tin oxide (ITO) plate was straightforward, suggesting that this POSS derivative could be applied as a component of polymer light emitting diodes (PLEDs).[42,43]

Figs. 1 and 2 present the WXRD, TGA and DSC data, respectively, of Cz-C11ene and POSS-C11-Cz. Cz-C11ene exhibits several sharp WXRD peaks because of its crystallinity. Surprisingly, the attachment of Cz-C11ene to the POSS core led to the disappearance of these sharp peaks, which were replaced by a peak at a low angle (6.63°) and a broad amorphous halo appearing at 18.31°, indicating that the crystalline Cz-C11ene became non-crystalline after its attachment to the POSS cage. Moreover, the *d*-spacing of 1.33 nm (6.63°), which is close to the calculated molecular size of the attached C11-Cz segment, suggest the existence of interpenetration between the C11-Cz segments [44–48]. In the DSC curves in Fig. 2, Cz-C11ene exhibits a sharp melting point (T_m) at 115 °C, whereas POSS-C11-Cz displays a clear glassy transition ($T_g = 45$ °C),

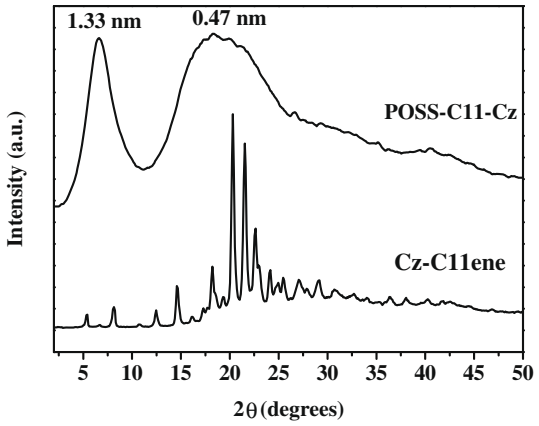

Fig. 1. WXRD data for POSS-C11-Cz and Cz-C11ene.

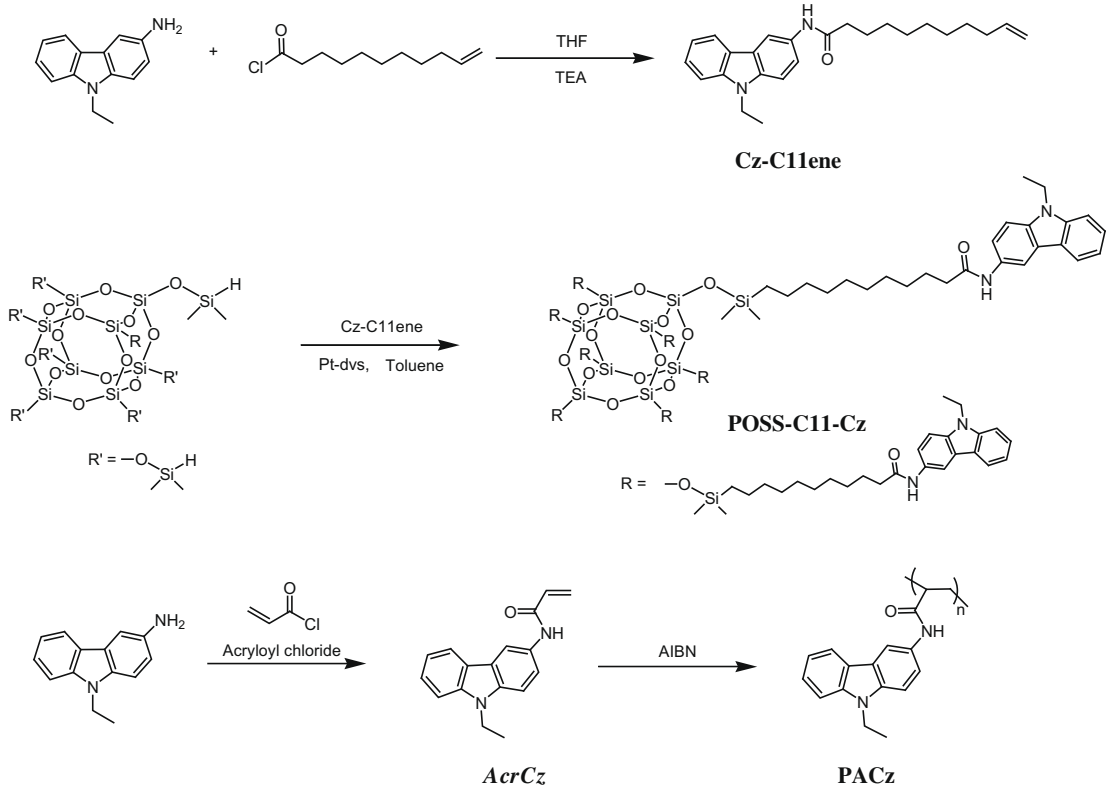

Scheme 1. Synthetic procedures used to obtain POSS-C11-Cz and PACz.

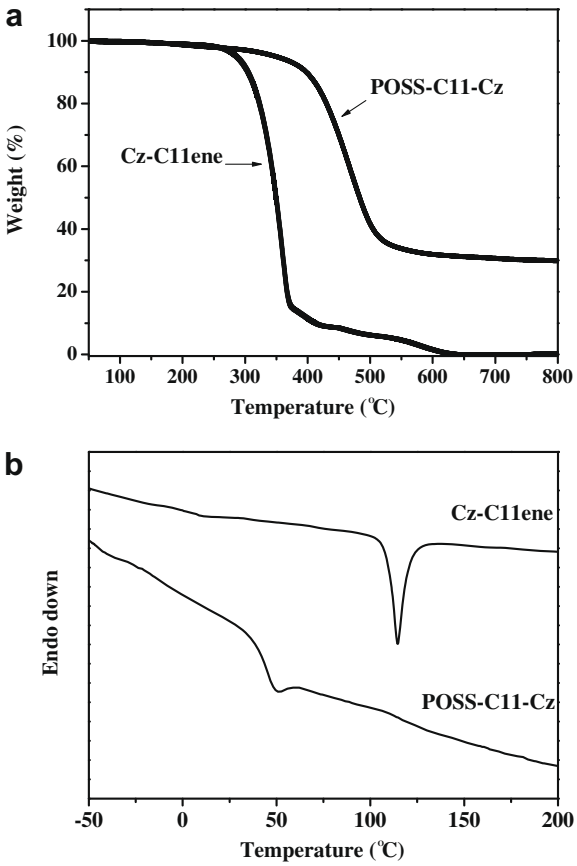

Fig. 2. (a) TGA and (b) DSC curves of POSS-C11-Cz and Cz-C11ene.

indicating that the attachment of Cz-C11ene units to the POSS cage led to a reduction in the packing of its molecular chains [25,49]. The TGA curves of POSS-C11-Cz and

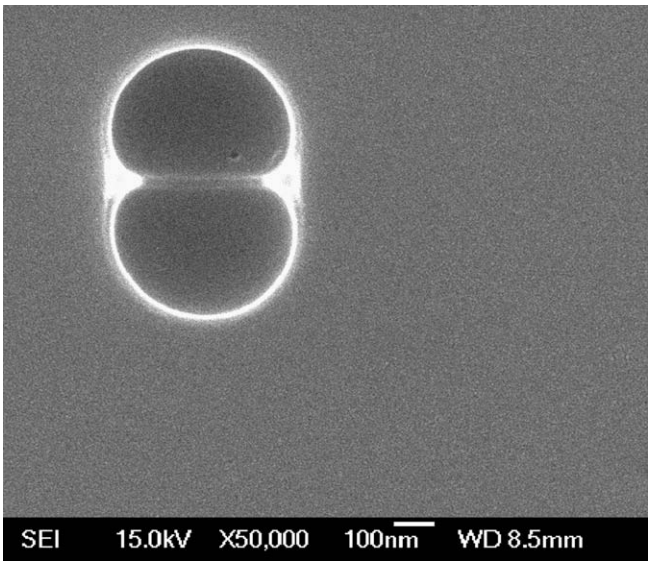

Fig. 3. SEM image of POSS-C11-Cz; removal of the solvent caused a bubble, which appears in the form of a light circle.

Cz-C11ene (Fig. 2) reveal thermal decomposition temperatures (T_d, 5 wt.% loss) of 350 and 286 °C, respectively. The ceramic yield of POSS-C11-Cz at 800 °C was 30% against the theoretical value of 26%. The unreacted carbon that was present could account for higher than expected ceramic yield, indicating its superior thermal stability.

Previous studies [19,25,50–52] revealed that the diameters of POSS derivatives containing organic chromophores are equal to or greater than 1.2 nm, and that bonding to nanosized POSS cages interrupts the aggregation of these chromophores units, resulting in a reduction of the

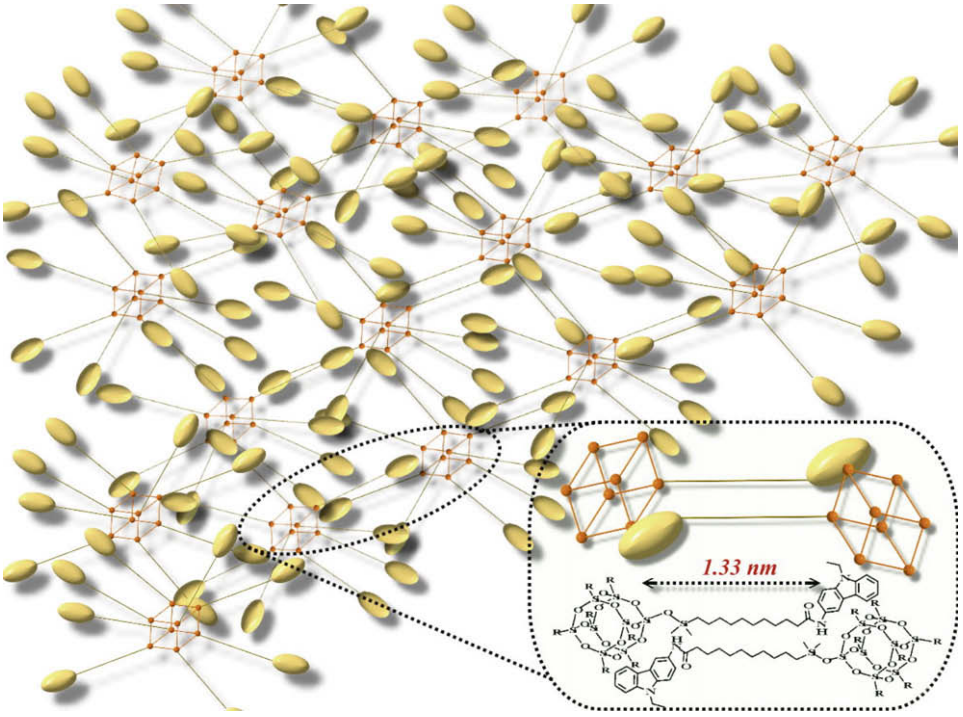

Scheme 2. Graphical representation of the well-ordered dispersive structure formed from POSS-C11-Cz in bulk state.

crystallinity of light-emitting materials, thereby improving PL and EL efficiencies [53]. The SEM image in Fig. 3 indicates that POSS-C11-Cz was well dispersed, as depicted in Scheme 2.

3.2. Electrochemical, optical and electroluminescence properties of POSS-C11-Cz

We anticipated that POSS-C11-Cz, which contains eight 3,9-carbazole groups, would exhibit improved electrochemical stability of its carbazole units [26,54–57]. Fig. 4 displays the cyclic voltammogram of POSS-C11-Cz, indicating that the attachment of 3,9-carbazole units to the POSS cage did not change its original circuit potential appreciably, i.e. it exhibits high electrochemical stability. Thus, the presence of the POSS cage did not affect the electrochemical properties of 3,9-carbazole [58].

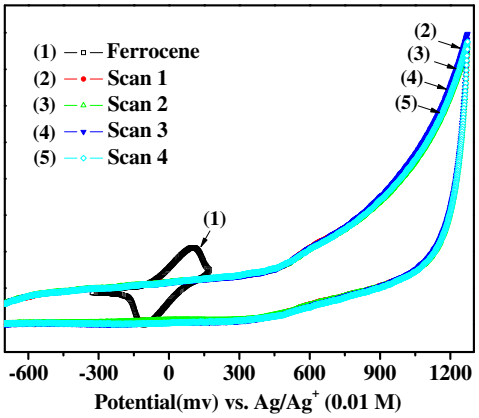

Fig. 4. Cyclic voltammagrams of POSS-C11-Cz.

Fig. 5 presents the UV–vis and PL spectra of POSS-C11-Cz and PACz in chloroform; the wavelengths of maximum absorption of both POSS-C11-Cz and PACz were 346 nm in their UV–vis spectra and 390 nm in their PL spectra. The shape of the PL emission spectrum of POSS-C11-Cz is substantially different from that of PACz. The emission wavelength was blue-shifted most likely because the POSS cage interrupts the aggregation of the chromophore groups [19]. The PL quantum efficiency (Q) of POSS-C11-Cz in chloroform, estimated in reference to 9,10-diphenylanthrancene ($Q = 0.90$), was 0.19, nearly identical to that of Cz-C11ene ($Q = 0.20$) but substantially higher than that of PACz ($Q = 0.10$) in a PVK-based polymer [59]. Carbazole groups attached to POSS-Cz-C11 appear to be well separated by the POSS cage and the long alkyl chain linkers; thus, the formation of excimers, which decrease the quantum yield, was effectively suppressed.

Fig. 5 displays the UV–vis and PL spectra of POSS-C11-Cz and PACz in the solid state; again, POSS-C11-Cz and PACz exhibit the same maximum absorptions in their UV–vis (at 348 nm) and PL spectra (at 390 nm). The maximum PL emission of POSS-C11-Cz in the solid state coincides with that in solution, whereas PACz exhibits a main peak at 390 nm accompanied by a shoulder at ca. 460 nm, implying that the tendency toward forming an inter-chain excimer formation (460 nm) was decreased and that aggregation of both the inter-chain and chromophoric segments was also reduced by the presence of the POSS cages.

Fig. 6 displays the excitation/emission (ex-em) measurements of POSS-C11-Cz; the excitation and emission peaks are nearly symmetric at 369 nm for the UV–vis spectrum and at 388 nm for the PL spectrum, respectively. This

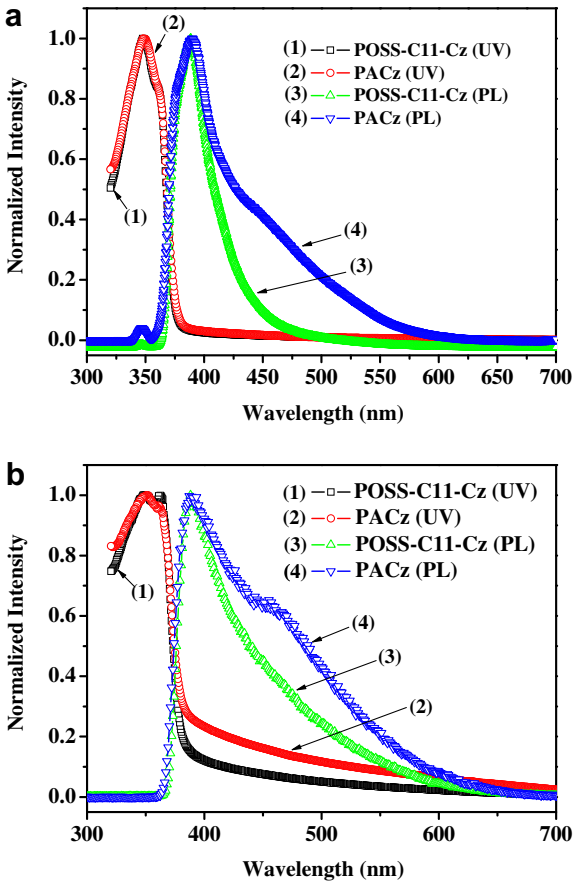

Fig. 5. UV–vis absorption and PL emission spectra of POSS-C11-Cz and PACz in (a) chloroform solution and (b) the solid state.

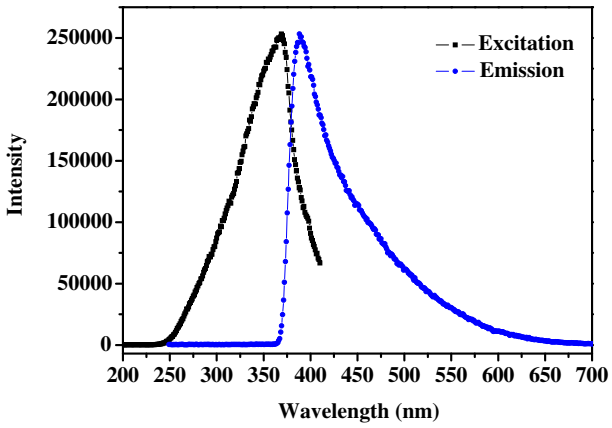

Fig. 6. Excitation and emission spectra of POSS-C11-Cz.

result indicates that the POSS cage simultaneously suppresses aggregation of the chromophore groups and enhances the color stability of the 3,9-carbazole units in the solid state [22,26].

The electroluminescence of POSS-C11-Cz in a PLED is deep blue. We assembled the device through sequential coating of PEDOT (to improve the hole injection), POSS-C11-Cz (emissive layer), TPBI (electro-transport material), LiF (electrode) and Al layers onto ITO (transparent anode) [i.e. ITO/PEDOT/POSS-C11-Cz or PACz (ca. 60 nm)/TPBI/LiF/Al] [36]. Fig. 7a and b displays plots of the current density and brightness with respect to the voltage from the device.

The turn-on voltage and maximum EL peak ($\lambda_{EL\text{-}max}$) of the POSS-C11-Cz-based device were 5.2 ± 0.1 V and 423 ± 1 nm, respectively; the maximum brightness was 45 cd m^{-2} at 11 V; the maximum external quantum efficiency was 0.06% at a current density of 4.3 mA cm^{-2}. The maximum external quantum efficiency of the PACz-based device was 0.02% at a current density of 5.9 mA cm^{-2}. The POSS-C11-Cz-based device exhibited a higher maximum external quantum than did the PACz-based device because the POSS cages separate the attached carbazole groups and suppress aggregation. Interestingly, the maximum brightness of the EL obtained from a POSS-C11-Cz (3 wt.%)/PACz (97 wt.%) blend was twice that of the PACz-based device, and the turn-on voltage was reduced from 10.5 to 7.5 V. Thus, a small amount POSS-C11-Cz acted as an effective dopant to transfer energy to PACz; therefore, POSS-C11-Cz appears to have potential for use in improving the quantum efficiency and color stability of polyfluorenes through blending [33–39].

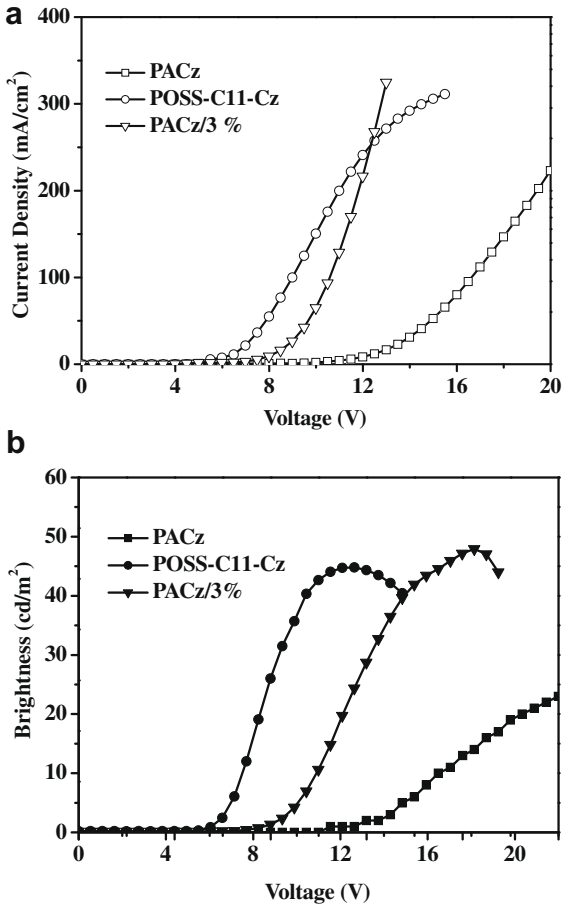

Fig. 7. (a) Voltage–current density (V–I) and (b) voltage–luminance (V–L) characteristics of devices having the configurations ITO/PEDOT/emissive layer/TPBI/LiF/Al.

3.3. Photoluminescence and PLED manufactured through a POSS-C11-Cz/polyfluorene blend

Polyfluorenes are promising candidates for blue-light emitting materials because of their high PL efficiency, EL efficiency and thermal stability [60–62]. Nevertheless, red-shifted emissions – attributed to either intermolecular interactions leading to the aggregation or the emissive keto defect sites caused by the thermo- or electro-oxidation of the polyfluorene backbone – limits their applications in PLEDs [33–39].

Consistent with the results described in the section above, we found that a device manufactured by incorporating a small amount of POSS-C11-Cz into poly(9,9′-dioctylfluorene) (POF) exhibited significantly improved color stability and EL properties. After heating a film composed of POSS-C11-Cz and POF, we measured the effect of the incorporation of POSS-C11-Cz on the photoluminescence properties of POF. The PL spectra (Fig. 8) reveal that the green emission peak at 530 nm of the POSS-C11-Cz (3%)/POF (97%) blend in the solid state had a lower intensity than that of the POF polymer itself. The PL stability of this blend is similar to that of other polyfluorene derivatives [20,63–67], indicating that incorporation of POSS-C11-Cz into POF polymer reduces the extent of both aggregation and keto defects of the POF. Fig. 9 presents plots of the external quantum efficiency with respect to the current density and the EL spectra of the POF- and POSS-C11-Cz/POF-based triple-layer LED devices mentioned above. The incorporation of POSS-C11-Cz did not

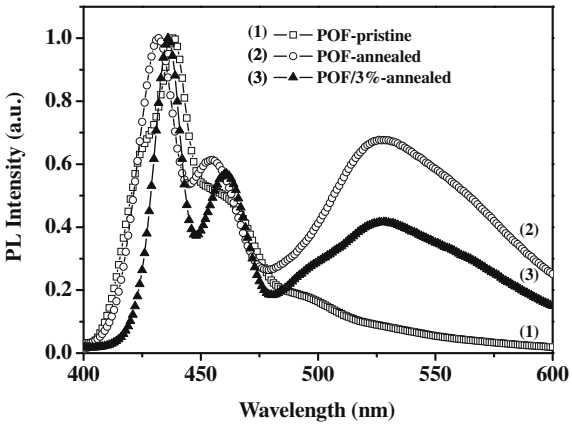

Fig. 8. PL spectra of spin-coated films of pristine POF, annealed POF and annealed POF/3% POSS-C11-Cz; annealing conditions: 200 °C, 5 h.

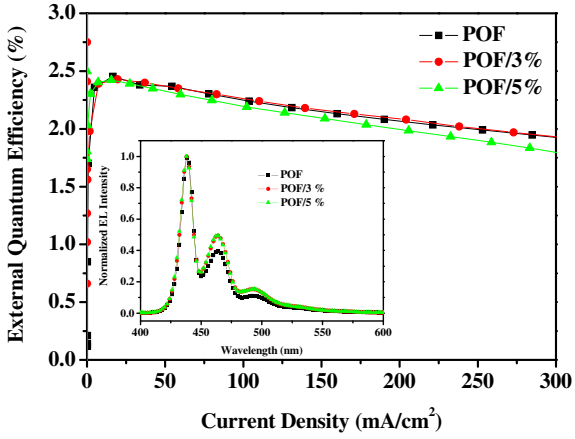

Fig. 9. EL spectra and voltage – external quantum efficiency characteristics of POSS-C11-Cz/POF-based devices.

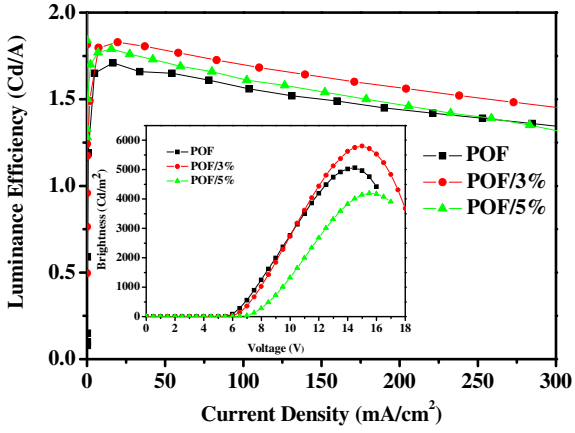

Fig. 10. Voltage–luminance (V–L) and current density–luminance efficiency characteristics of POSS-C11-Cz/POF-based devices.

appreciably change the EL and quantum efficiencies of the POF. However, the POSS-C11-Cz (3 wt.%)/POF (97 wt.%)-based device exhibited higher maximum brightness and luminance efficiency than did the POF-based device because of the doping effect of POSS-C11-Cz (Fig. 10) [68], which enhanced energy transfer efficiency from the carbazole chromophore groups on POSS-C11-Cz to POF and suppressed the aggregation of POF. The brightness of the POSS-C11-Cz/POF-based device decreased slightly upon increasing the POSS-C11-Cz content to 5 wt.% because of an increase in the resistivity of the light emitting layer. The compatibility of POSS-C11-Cz and POF was also responsible for this deterioration in brightness.[69] We are currently investigating the mechanism of deterioration caused by the addition of POSS-C11-Cz.

4. Conclusions

In summary, we have synthesized, in high yield, a novel POSS derivative (POSS-C11-Cz) containing eight blue-light electroluminescent functionalities. This novel POSS derivative has good thermal stability, electrochemical stability and film-forming properties. From optical and electroluminescence measurements, we found that attachment to the POSS cage suppressed aggregation and enhanced the color stability of 3,9-carbazole units both in solution and in the solid state. POSS-C11-Cz also behaves as an effective dopant that enhances energy transfer from itself to POF. In addition, POSS-C11-Cz improves the quantum efficiency and color stability of POF because its presence reduces the degree of aggregation and the formation of keto defects. A POSS-C11-Cz (3 wt.%)/POF (97 wt.%)-based device exhibited higher maximum brightness and luminance efficiency than did the non-blended POF-based device.

Acknowledgements

This study was supported financially by the Ministry of Education's "Aim for the Top University" (MOEATU) program and by the National Science Council, Taiwan (Contract No. NSC-96-2218-E-009-008).

Appendix A. Supplementary data

Supplementary data associated with this article can be found, in the online version, at doi:10.1016/j.actamat.2008.12.031.

References

[1] Choi J, Tamaki R, Kim SG, Laine RM. Chem Mater 2003;15:3365.
[2] Livage J. Bull Mater Sci 1999;22:201.
[3] Choi J, Kim SG, Laine RM. Macromolecules 2004;37:99.
[4] Choi J, Yee AF, Laine RM. Macromolecules 2004;37:3267.
[5] Tamaki R, Choi J, Laine RM. Chem Mater 2003;15:793.
[6] Bassindale AR, Liu Z, MacKinnon IA, Taylor PG, Yang Y, Light ME, et al. Dalton Trans 2003:2945.
[7] Zhang L, Abbenhuis HCL, Yang Q, Wang YM, Magusin PCMM, Mezari B, et al. Angew Chem Int Ed 2007;46:5003.
[8] Phillips SH, Haddad TS, Tomczak SJ. Curr Opin Solid State Mater Sci 2004;8:21.
[9] Jeoung E, Carroll JB, Rotello VM. Chem Commun 2002:1510.
[10] Neumann D, Fisher M, Tran L, Matisons JG. J Am Chem Soc 2002;124:13998.
[11] Sanchez C, Soler-Illia GJAA, Ribot F, Lalot T, Mayer CR, Cabuil V. Chem Mater 2001;13:3061.
[12] Pyun J, Matyjaszewki K. Chem Mater 2001;13:3436.
[13] Schubert U. Chem Mater 2001;13:3487.
[14] Wu G, Su Z. Chem Mater 2006;18:3726.
[15] Lu SY, Hamerton I. Prog Polym Sci 2002;27:1661.
[16] Costa ROR, Vasconcelos WL, Tamaki R, Laine RM. Macromolecules 2001;34:5398.
[17] Brick C, Tamaki MR, Kim SG, Asuncion MZ, Roll M, Nemoto T, et al. Macromolecules 2005;38:4655.
[18] Brick C, Ouchi MY, Chujo Y, Laine RM. Macromolecules 2005;38:4661.
[19] Xiao S, Nguyen M, Gong X, Cao Y, Wu H, Moses D, et al. Adv Funct Mater 2003;13:25.
[20] Lin WJ, Chen WC, Wu WC, Niu YH, Jen AKY. Macromolecules 2004;37:2335.
[21] Sellinger A, Tamaki R, Laine RM, Ueno K, Tanabe H, Williams E, et al. Chem Commun 2005:3700.

[22] Cho HJ, Hwang DH, Lee JI, Jung YK, Park JH, Lee J, et al. Chem Mater 2006;18:3780.
[23] Lo MY, Zhen C, Lauters M, Jabbour GE, Sellinger A. J Am Chem Soc 2007;129:5808.
[24] Froehlich JD, Young R, Nakamura T, Ohmori Y, Li S, Mochizuki A, et al. Chem Mater 2007;19:4991.
[25] Xiao Y, Liu L, He CB, Chin WS, Lin TT, Mya KY, et al. J Mater Chem 2006;16:829.
[26] Imae I, Kawakami Y. J Mater Chem 2005;15:4581.
[27] Chen WY, Ho KS, Hsieh TH, Chang FC, Wang YZ. Macromol Rapid Commun 2006;27:452.
[28] Lin HC, Kuo SW, Huang CF, Chang FC. Macromol Rapid Commun 2006;27:537.
[29] Liu YL, Chang GP, Hsu KY, Chang FC. J Polym Sci A Polym Chem 2006;44:3825.
[30] Lee YJ, Kuo SW, Huang CF, Chang FC. Polymer 2006;47:4378.
[31] Lin HM, Wu SY, Huang PY, Huang CF, Kuo SW, Chang FC. Macromol Rapid Commun 2006;27:1550.
[32] Chan SC, Kuo SW, Chang FC. Macromolecules 2005;38:3099.
[33] Liu R, Xiong Y, Zeng W, Wu Z, Du B, Yang W, et al. Macromol Chem Phys 2007;208:1503.
[34] Kulkarni AP, Kong X, Jenekhe SA. J Phys Chem B 2004;108:8689.
[35] Bazan GC, Heeger AJ, Xiao SS. Adv Funct Mater 2003;13:325.
[36] Culligan SW, Geng Y, Chen SH, Klubek K, Vaeth KM, Tang CW. Adv Mater 2003;15:1176.
[37] Panozzo S, Vial JC, Kervella Y, Stephan O. J Appl Phys 2002;92:3495.
[38] List EJW, Guentner R, Scanducci de Freitas P, Scherf U. Adv Mater 2002;14:374.
[39] Lupton JM, Craig MR, Meijer EW. Appl Phys Lett 2002;80:4489.
[40] Burda C, Chen X, Narayanan R, El-Sayed MA. Chem Rev 2005;105:1025.
[41] Cui Y, Liu C, Gao Q. Polym Adv Technol 2000;11:172.
[42] Choulis SA, Choong VE, Patwardhan A, Mathai MK, So F. Adv Funct Mater 2006;16:1075.
[43] van Woudenbergh T, Wildeman J, Blom PWM, Bastiaansen JJAM, Langeveld-Vos BMW. Adv Funct Mater 2004;14:677.
[44] Witten TA, Leibler L, Pincus P. Macromolecules 1990;23:824.
[45] Semenov AN. Macromolecules 1992;25:4967.
[46] Chen HL, Hsiao MS. Macromolecules 1999;32:2967.
[47] Ruokolainen J, ten Brinke G, Ikkala O. Macromolecules 1996;29:3409.
[48] Milner ST, Witten TA, Cates ME. Macromolecules 1998;21:2610.
[49] Carroll JB, Waddon AJ, Nakade H, Rotello VM. Macromolecules 2003;36:6289.
[50] Laine RM. J Mater Chem 2005;15:3725.
[51] Jenekhe SA, Zhang X, Chen XL, Choong VE, Gao Y, Hsieh BR. Chem Mater 1997;9:409.
[52] Alam MM, Tonzola CJ, Jenekhe SA. Macromolecules 2003;36:6577.
[53] Kraft A, Grimsdale AC, Holmes AB. Angew Chem Int Ed 1998;37:402.
[54] Kanega H, Shirota Y, Mikawa H. J Chem Soc Chem Commun 1984:158.
[55] Nawa K, Imae I, Noma N, Shirota Y. Macromolecules 1995;28:723.
[56] Taranekar P, Huang C, Fulghum TM, Baba A, Jiang G, Park JY, et al. Adv Funct Mater 2008;18:347.
[57] Grell M, Bradley DDC, Ungar G, Hill J, Whitehead KS. Macromolecules 1999;32:5810.
[58] Lee J, Cho HJ, Jung BJ, Cho NS, Shim HK. Macromolecules 2004;37:8523.
[59] Yokoyama M, Tamamura T, Atsumi M, Yoshimura M, Shirota Y, Mikawa H. Macromolecules 1975;8:101.
[60] Babel A, Jenekhe SA. Macromolecules 2003;36:7759.
[61] Scherf U, List EJW. Adv Mater 2003;14:477.
[62] Neher D. Macromol Rapid Commun 2001;22:1365.
[63] Chou CH, Hsu SL, Dinakaran K, Chiu MY, Wei KH. Macromolecules 2005;38:745.
[64] Wu FI, Reddy DS, Shu CF, Liu MS, Jen AKY. Chem Mater 2003;15:269.
[65] Shu CF, Dodda R, Wu FI, Liu MS, Jen AKY. Macromolecules 2003;36:6698.
[66] Cho HJ, Jung BJ, Cho NS, Lee J, Shim HK. Macromolecules 2003;36:6704.
[67] Lim E, Jung BJ, Shim HK. Macromolecules 2003;36:4288.
[68] Zheng T, Choy WCH. J Phys D Appl Phys 2008;41:1.
[69] Chappell J, Lidzey DG, Jukes PC, Higgins AM, Thompson RL, O'Connor S, et al. Nat Mater 2003;3:616.
[70] Grell M, Bradley DDC, Inbasekaran M, Woo EP. Adv Mater 1997;9:798.
[71] Su HJ, Wu FI, Tseng YH, Shu CF. Adv Fun Mater 2005;15:1209.
[72] Chien CH, Shih PI, Wu FI, Shu CF, Chi Y. J Polym Sci A Polym Chem 2007;45:2073.